Mineral Proximity Influences Mechanical Response of Proteins in Biological Mineral−Protein Hybrid Systems

Pijush Ghosh, Dinesh R. Katti and Kalpana S. Katti*

Department of Civil Engineering, North Dakota State University, Fargo, North Dakota 58105

Received September 30, 2006; Revised Manuscript Received December 12, 2006

The organic phase of nacre, which is composed primarily of proteins, has an extremely high elastic modulus as compared to that of bulk proteins, and also undergoes large deformation before failure. One reason for this unusually high modulus could be the mineral−organic interactions. In this work, we elucidate the specific role of mineral proximity on the structural response of proteins in biological structural composites such as nacre through molecular modeling. The "glycine-serine" domain of a nacre protein Lustrin A has been used as a model system. It is found that the amount of work needed to unfold is significantly higher when the GS domain is pulled in the proximity of aragonite. These results indicate that the proximity of aragonite has a significant effect on the unfolding mechanisms of proteins when pulled. These results will provide very useful information in designing synthetic biocomposites, as well as further our understanding of mechanical response in structural composites in nature.

Introduction

The mechanical response of organics in their innate forms in biology is often significantly different from that in their pure extracted forms tested in the laboratory. One example of this is exhibited by the organic phase in the 20 nm space between the 200−400 nm aragonitic mineral platelets in nacre found in many molluscan shells. The elastic modulus of the organic layer obtained is shown to be of the order of 15−20 GPa from simulation results[1] and nanoindentation tests.[2] Nacre, the shiny inner layer of molluscan seashells, is widely investigated as a model biomimetic system for the design of next generation advanced materials. The fracture toughness of nacre is about 3 orders of magnitude higher than monolithic ceramics, and its strength is among the highest in shell structures.[3] In literature, the structure of nacre[4,5] and the influence of different microstructural features on its mechanical properties have been studied.[6−8] Our prior work has revealed that the organic present in nacre shows high elastic modulus of about 15−20 GPa and at the same time has the ability to undergo large deformation before failure.[2,6] The organic phase in nacre appears to have significant differences in properties as compared to bulk proteins both in terms of exhibiting a very high elastic modulus and simultaneously the ability to undergo large deformations. These differences in characteristics of the nacre-organic could be hypothesized to be because of two major reasons: the mineral−organic interactions, and confinement of organics between the platelets.

The focus of this work is to study the mineral−organic interactions and the effect of mineral on protein unfolding. Structural composites in nature, such as bone, teeth, and seashells, are often hybrid systems of proteins and minerals. In this work, we focus specifically on how the mineral−protein interaction influences the mechanical response of protein in a biocomposite material.

Significant research has been done in understanding the role of water[9−13] in biological systems such as protein−enzyme interaction, folding−unfolding, etc. In a recent study, the influence of water on the functional behavior of α helix has been evaluated using atomistic simulation.[14] The nature of water in nacre also has been the subject of recent studies.[15−17] It seems reasonable to believe that water has an important role to play in the mechanical behavior of proteins. A clear understanding of the deformation mechanisms involved in the folding−unfolding behavior of proteins at mineral proximity along with the knowledge of the role of "biological water" in the mechanical behavior of protein could enhance the understanding of structural biological materials and in turn could lead to a successful design of new biomaterials or biomimetic materials.

We have used Steered Molecular Dynamics (SMD) for these studies. A model protein domain structure, based on proteins in nacre, is used. The glycine-serine (GS) domain of the protein Lustrin A from nacre has been used as a model for organics. The mineral component in the simulations is aragonite, the mineral constituent of nacre. The influence of mineral proximity on mechanical response of protein is studied.

Model Construction

Mineral. Aragonite is a carbonate mineral that is a polymorph of calcite. The unit cell structure for aragonite is obtained from the American Mineralogist Crystal Structure Database.[18] The unit cells are patched by PSFGEN module of NAMD[19] to build a larger structure. The aragonite model extends 16 unit cells in the *x*-direction, 16 in the *y*-direction, and 2 unit cells in the *z*-direction.

Organic. In nacre, 3−5% of organics are primarily proteins, with some glycoproteins and chitin[20,21] playing a critical role in the functional and behavioral properties of nacre. Different proteins derived from different species of seashells are reported to have different properties and perform different functions in nacre. Some of these provide the nucleation sites for the growth of aragonite crystals,[22] and some are responsible for the secretion of calcium carbonate polymorphs,[23,24] whereas many of them play a key role in stabilizing the aragonite crystal arrangement.[25] Most of these proteins mentioned are known to have a single functionality. Lustrin A from Haliotis Rufescens, which is the most widely studied, is a large multidomain protein

* Corresponding author. E-mail: kalpana.katti@ndsu.edu.

10.1021/bm060942h CCC: $37.00
Published on Web 02/22/2007

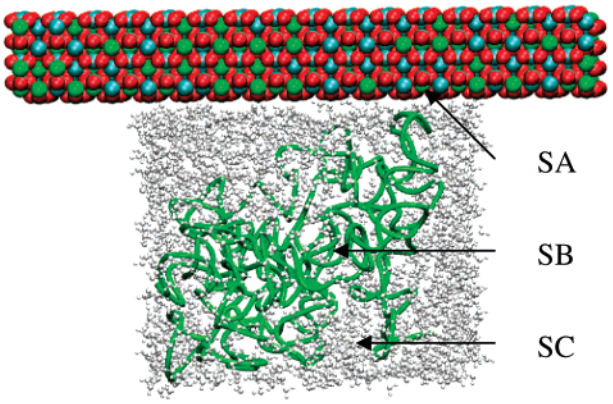

Figure 1. The aragonite GS combined model showing different segments. SA, aragonite; SB, GS domain; SC, water.

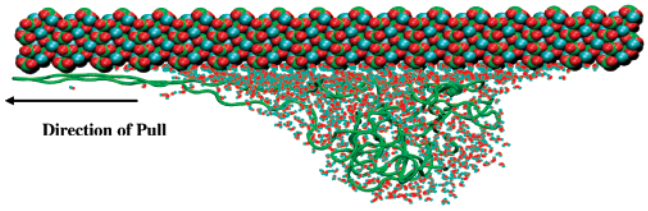

Figure 2. Model of GS domain at mineral proximity as the GS domain is pulled. The ball form with the cyan, red, and green combination is atoms in aragonite, the ribbon form in green is the GS domain, and the line form with red and cyan lines represents water.

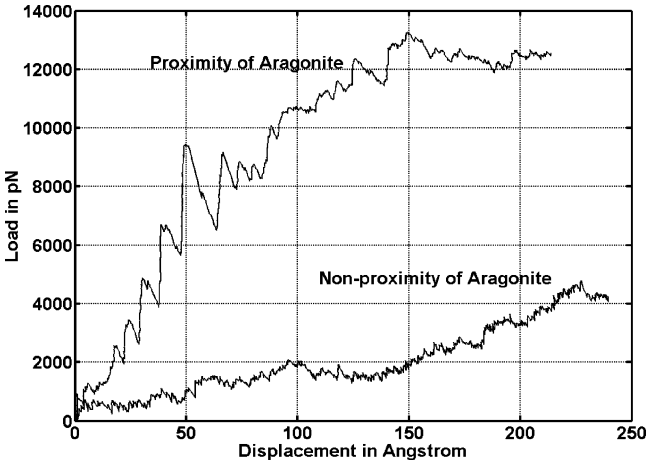

Figure 3. Load−displacement (L−D) characteristics of the organic entity (GS domain) in the presence and absence of mineral aragonite.

known to perform several functions.[26] Analysis of its modular structure reveals that it has 10 cysteine-rich domains (C1−C10), with eight proline-rich domains (P1−P8) sitting between each of these cysteine domains, acting as an extender, allowing them to work independently. Shen et al. have shown that the cysteine domain controls the mineralization of nacre.[27] The primary role of the proline domains is to act as spacers between cysteine domains. The arginine- and lysine-rich basic residues at the end of the cysteine domain have potential to interact with the anionic molecule during the shell formation.

Lustrin A has a domain of 275 residues, of which 250 are either glycine (G) or serine (S). This is one of the largest discrete structural domains in Lustrin A. The secondary structure analysis of this domain indicates that it is rich in "turns". This domain is also rich in glycine loops.

These types of domains find close homology with proteins such as keratin and loricrin.[28] As suggested by Shen et al., this type of domain possesses high elastic property that enables it to function as an extensor molecule. Zhang et al. have shown that elastic (GS)*x* and (GSSS)*y* "serine loops", which are characteristics of this domain, could protect the aragonite mineral phase from fracture or separation.[29] Functional and structural homology study of this domain leads to the understanding that this domain has significant structural contribution as far as the overall behavior of the whole protein Lustrin A is concerned. Because the whole Lustrin A protein is very large in size and its complete structure is not known, we have used the GS domain as a model system to study the influence of mineral aragonite on the structural response of organic. The GS domain isolated from the primary structure of Lustrin A is used in this study. The GS model is then solvated using the "SOLVATE" module of VMD,[30] and the type of water model used is TIP3. The primary sequence of the GS domain is as follows:

GSGSGSGSGSGSGSSSSSSSGSTSGSGSGSGSGSSSGS-GSGSSSASGSGSG SGSSSASGSGSSSGSGSGSSSGSG-SGSGSGSGSSSGSSSVSNSWTGSGSSSGS GSGSSSWS-GSSSGTGSGSSSWFGSGSSGSGSDSSSGSSSASGSGSSSG-SSSGS GSGSSLWFGSGSSSGTGSGSSSGSSSGSGSD-SSSGSTSGSSSGSGSASGSGTG S.

The tertiary structure of this GS domain is also unknown, and it is extremely difficult to predict its structure from its homologous proteins, the structure of which is not completely known either. We have hence generated a random structure based on its primary sequence. The random structures are generated using molecular modeling software SYBYL and provide a model system for the simulations.

For building the aragonite−organic hybrid model, the solvated GS model is placed next to aragonite in the *x*−*y* plane. The aragonite−GS combined model used in this study is shown in Figure 1. As shown, the three molecules are indicated by three segments SA, SB, and SC, which represent the mineral, aragonite, the organic, GS, and solvent, water, respectively. The total number of atoms in the model is 17 617 with 2139 representing the GS domain, 5238 for the water, and 10 240 for aragonite.

Table 1. Work Factor Obtained at Various Velocities

velocities (Å/ps)	work factor
0.25	10.50
0.50	8.50
1.00	5.00

Simulation Details

SMD and various experimental techniques have been extensively used in the past to study the unbinding of proteins and other biological molecules under various conditions.[31−33] Here, SMD simulations are performed on the GS domain both in the proximity and in the absence of aragonite. One of the α carbon atoms of the backbone chain is pulled while keeping another α carbon on the other part of the domain fixed. The structures are minimized, raised to room temperature, and pressure followed by equilibrating before any pull is applied.

The GS domain is pulled at three different velocities of 0.25, 0.50, and 1.00 Å/ps. Although it is desirable to choose velocities for protein pulling matching velocities expected in the real world or experimental environment, at the current time, due to constraints on simulation duration imposed by even the state of the art computational resources, SMD modelers attempt to

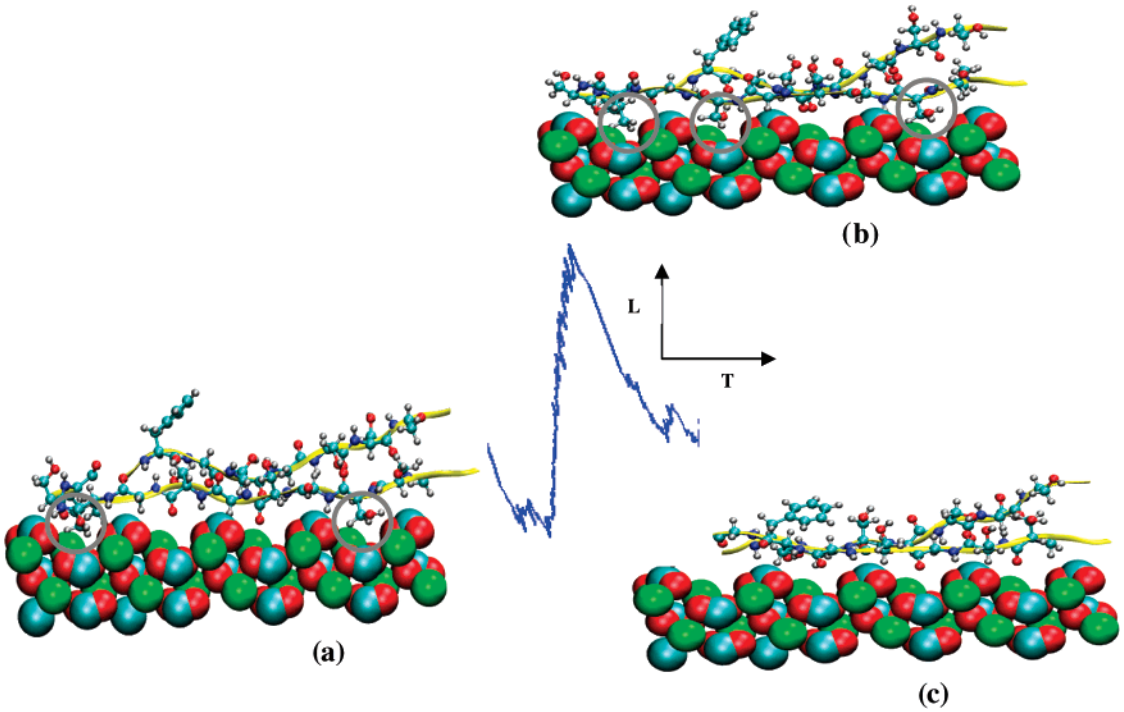

Figure 4. Snapshots showing interactions between protein and mineral atoms corresponding to the beginning, apex, and end of a peak on the load deformation curve. (a) Beginning of the peak, (b) apex, and (c) end of the peak of the L−D curve. The ball form is aragonite, where cyan, red, and green are carbon, oxygen, and calcium, respectively. The CPK (Corey, Pauling, and Kultin) and ribbon form together represent a strand of organic, where white is hydrogen, red is oxygen, cyan is carbon, and blue is nitrogen.

pull proteins through a predetermined amount of displacement rather than attempting to match velocities. In the present work, we have used a range of velocities and duration of 250 ps. The stiffness of the SMD spring used is 5 kcal/mol/Å^2. The pull test under each velocity is conducted a minimum of three times. The parameters for organic GS are obtained from CHARMm parameter file pro_all_para.in.[34] For aragonite, the parameters for the bonded parts are directly used from existing literature. For the nonbonded energy expression, Buckinghum potential was used in the past, and thus parameters are available. The parameters for 12-6 Lennard-Jones nonbonded potential in the CHARMm force field are derived from available parameters. The SMD simulations are run for 250 ps in each case, with 1 fs time step. This duration of pulling results in displacement in the range of 50−230 Å. The choice of minimum displacement was based on the mechanical response of nacre and our previous finite element modeling simulations. Our calculations indicate that, within the elastic displacement range of nacre, the relative displacement between the aragonite platelets and the organic phase could be as much as 50 Å. All simulations are conducted in the isobaric−isothermal, constant number, pressure, and temperature (NPT) ensemble. Periodic boundary condition has been applied with appropriate box size. The particle mesh Ewald (PME) technique has been used to calculate the electrostatic interaction energy. The simulations were conducted on the TeraGrid supercomputer network and specifically the National Center for Supercomputing Application's cobalt SGI Altix supercomputing cluster.

Results and Discussion

The glycine-serine (GS) domain, which is extracted from nacre protein Lustrin A, is pulled under two different environments. In one case, the protein domain is pulled in the proximity of mineral aragonite as shown in Figure 2, and in the other case in the absence of the mineral. Further, the load deformation response of these two cases is analyzed to evaluate the effect of mineral proximity. The load−displacement (L−D) behavior of the GS domain for the two conditions is shown in Figure 3. The area under this L−D curve provides a good estimate of the amount of energy necessary to be expended to unfold an organic entity by a certain magnitude of displacement. Here, we define a term "work factor", which is equal to the ratio of work done at mineral proximity to the work done without mineral proximity. The simulations were conducted at 1.00, 0.50, and 0.25 Å/ps velocities for duration of 250 ps in each case. The "work factor" obtained at the three different velocities is shown in Table 1. It is observed that the amount of work necessary to unfold the protein is about 10 times more when pulled at the proximity of aragonite than in its absence at a velocity of 0.25 Å/ps. It appears that the work factor decreases with increase in velocity. A high magnitude of "work factor" indicates a significant influence of mineral proximity on the mechanical response of proteins. The specific factors responsible for the influence of mineral proximity may be attributed to two major phenomena.

Mineral−Protein Interactions. *Dynamics of Protein−Solvent (Water) with Protein and Mineral.* As seen in Figure 3, the load−displacement (L−D) curve obtained when pulled in mineral proximity exhibits two major features: (i) large peaks and (ii) higher magnitudes of load in the L−D response as compared to protein alone. Detailed observation of the protein unfolding with and without the mineral present and conformation of the protein and water was made and compared to the load deformation response to understand the mechanisms responsible for each of the features. The unfolding mechanism observed and the L−D response without mineral is as expected and similar to the L−D curves reported in the literature from SMD simulations and AFM experiments. The peaks are of the order of 200−300 pN as a result of opening of loops and turns and

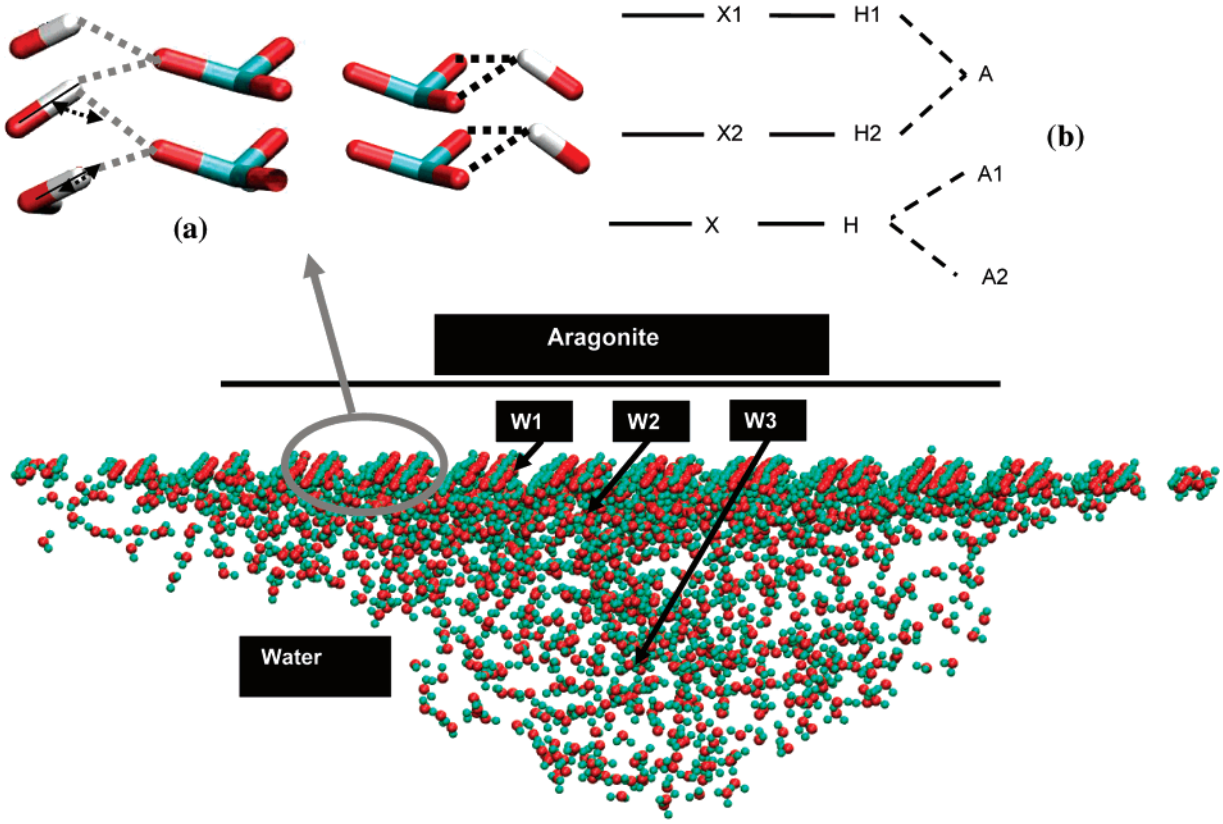

Figure 5. The conformation of the water molecules (biological water) as the GS domain is stretched at mineral proximity. W1 refers to water bound to the aragonite surface, W2 is water that is highly oriented, influenced by aragonite proximity, and W3 is the bulk water. The inset shows (a) the interaction of the water molecules with carbonate group of aragonite, and (b) two major hydrogen bond patterns observed at the interface between water molecules and aragonite. In the inset diagram, licorice with cyan and red is carbonate of aragonite, whereas red and white represent atoms in the water molecule.

breaking of hydrogen bonds and other bonds forming the conformation. However, in the presence of mineral, the peaks are significantly larger in magnitude at 1500−2000 pN and are fewer in frequency. Also, the magnitude of the force in the L−D curve is significantly higher for the case with mineral than the case without mineral.

As the protein is pulled parallel to the mineral surface, the side chains of the protein as well as the backbone begin to interact with the atoms on the mineral surface. As the protein is pulled, some of the protein atoms "latch on" to specific sites on the mineral because of strong attractive interactions. As the "pull" continues, the side chains that have "latched on" put up significant resistance, the loops and turns in this segment of the protein open almost completely, and most of the applied force goes to "break" the latched atoms. The force increases rapidly until the "latch" breaks and the force drops precipitously, resulting in a peak. The protein segment moves forward with its atoms seeking another attractive set of atoms in the mineral to latch on to. While significant loops and turns in the very close proximity of the mineral open, the local loops and turns in the remaining portion of the protein do not show big changes, but rather open slowly as the protein is pulled. Although we observe a significant drop in force when the latched atoms break away, the magnitude of force needed to pull the protein is still much higher than in the case of no mineral presence, indicating considerable interactions between the mineral and the protein.

As the protein pulling continues, some of the water molecules clustered around the solvated protein begin to disassociate from the protein and form first single and then multiple water layers between the protein and the mineral. As the thickness of water between the mineral and protein increases, the latching action between the protein atoms and the mineral atoms reduces, and then with increasing water layer thickness the latching action stops. The L−D curve becomes smooth with no large peaks. However, the magnitude of force needed to continue to pull the protein is still many times higher than the case without the mineral, indicating a continued significant influence of mineral on the protein and the water.

As mentioned above, the peaks in the L−D characteristics result from the "latch on" action between the protein and the aragonite molecule. This "latch on" action actually originates from the site-specific interaction of the side chains of protein with the surface atoms of aragonite. The interactions of the "latch on" phenomenon involved at each of the base points and the apex of the peak are shown in Figure 4. The water molecules are suppressed for clarity.

In our model, the GS domain is highly populated with serine, which has a $-CH_2OH$ functional group in its side chain. Two main sites of interactions are observed: the interaction between hydrogen of side chain, and the oxygen of carbonate groups of aragonite and the oxygen of $-CH_2OH$ with carbon of carbonate anion. Each of these peaks results from interaction of more than one site. Thus, the height and the base width of a peak depend primarily on the number of interaction sites and the closeness of the interacting groups. As observed in Figure 3, one peak is almost immediately followed by the other, and the reason attributed to this is the periodicity of the aragonite crystals, leading to a periodic symmetrical surface in the plane of pulling.

The van der Waals interactions between the aragonite and the organic are one of the major sources contributing to the

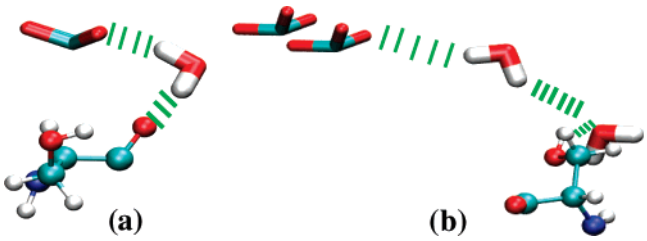

Figure 6. The hydrogen-bond bridging structure: (a) one water molecule is involved in bridging, and (b) two water molecules are involved in bridging. (i) The licorice with cyan and red is the carbonate group of aragonite, (ii) the licorice with white and red is the water molecule, and (iii) the CPK shows the residue of amino acid. (iv) Red, white, and cyan indicate oxygen, hydrogen, and carbon, respectively. The green lines show the hydrogen bond formation, maintaining necessary geometric conditions.

load as seen for the L−D curve. The other portion of the contribution comes from the characteristics of water as explained in the following section. It is observed that, as the organic is pulled, the van der Waals interaction between the aragonite and organic increases, thus bringing the two phases closer. Although the distance between the mineral surface and the bulk of the organic is more than 5 Å (usually after which this nonbonded interaction becomes weak), the number of atoms involved in this interaction is very large, thus resulting in a strong overall interaction.

As observed in the L−D curve, the slope of the curve is higher, and thus the curve is stiffer when pulled at mineral proximity. From the study with solvated and unsolvated protein and also from the conformation of water, it is clearly evident that water has a significant contribution in this mineral influence. The two likely ways water may contribute are by the change in the characteristics of water due to mineral proximity, and bridging by hydrogen bonds and nonbonded interactions.

In Figure 5, the conformation of water after the protein is pulled by a significant amount is shown. In the figure, W1, W2, and W3 are the rows formed by the water molecules close to the aragonite surface. From this figure, it is observed that the water molecules closest to the aragonite surface are highly orientated. The water loses this structure away from aragonite surface, and, at a distance of about 15 Å from the mineral surface, the orientation of water is random similar to bulk water. At the interface, water molecules form a strong hydrogen bond with the carbonate anions in two different patterns, shown in the inset of the Figure 5. The distribution of "r_1" and "θ_1" (the distance and angle of hydrogen) over ensemble of space shows a median value of 1.55 ± 0.08 Å and $166.5 \pm 5.8°$, respectively. This magnitude of distance and angle provides clear evidence of a strong hydrogen bond between water and carbonate molecules. From the analysis of the behavioral properties of protein water, for example, statics and dynamics of hydrogen bond, orientation, etc., it can be inferred that the presence of mineral makes the water molecules bind to the mineral or makes water less free to move. Thus, at mineral proximity, the protein is pulled through water, which behaves more structured and hence stiffer. In the absence of mineral proximity, protein water behaves as ordinary bulk water. The nonbonded interactions between aragonite and water molecules change the characteristics of the protein water, resulting in a need for more energy for pulling the protein through it.

Another important mechanism that causes the organic entity at mineral proximity to behave stiffer is the hydrogen bond bridging between aragonite, water, and protein. Figure 6 shows the bridging observed in this simulation. In some cases, the aragonite and organic are bridged through one water molecule, and in some cases two or more. This type of bridging structure makes the organic less liable to displace when pulled, thus contributing to the "work factor". The nonbonded interactions (including hydrogen bonding) between aragonite, water, and the protein play an important role in increasing the force required to pull the protein in the presence of the mineral after water enters between the mineral and protein.

Conclusions

The mechanical response of organic in nacre is significantly influenced by mineral proximity. At a given velocity, the amount of energy expended to unfold an organic domain by a certain magnitude of displacement is found to be several times more when pulled at mineral proximity than when pulled without mineral present. The factor by which additional amount of energy is required to unfold a protein domain at mineral proximity depends on the velocity with which the organic is pulled. This factor increases with decrease in velocity. The load displacement characteristics of organic at mineral proximity show higher peaks and also larger force magnitude for the same displacement when compared to one without mineral proximity. The peaks are also sharper. These peaks appear to be caused due to the site-specific interactions between the protein and the aragonite surface. The occurrences of large peaks disappear with increased deformation as water-surrounding protein gets between the aragonite and protein and inhibits direct site-specific interactions between the protein and the aragonite. The water surrounding the protein at the mineral protein interface becomes highly oriented. Despite the water between the protein and mineral, the magnitude of force required to pull the protein is many times larger than for the case without the mineral. For the first time, mechanical behavior of protein macromolecule in the proximity of mineral is studied. The interplay between mineral and proteins and alteration of the protein behavior, as a result, provide clues to some of the unique properties exhibited by the organic phase in biological nanocomposites, as in the case of nacre.

Acknowledgment. We acknowledge the TeraGrid allocation (TG-DMR060001T) and the NCSA Supercomputing Center for computational resources. This work was partially supported by National Science Foundation grant no. 0115928. Dr. Ken Chong was the program manager. We also acknowledge the use of the computational resources at the NDSU Center for High Performance Computing (CHPC) and Biomedical Research Infrastructure Network (BRIN), and Dr. Gregory Wettstein for hardware and software support for NAMD at NDSU. P.G. acknowledges support from ND EPSCOR.

References and Notes

(1) Katti, D. R.; Katti, K. S. *J. Mater. Sci.* **2001**, *36*, 1411.
(2) Katti, K. S.; Mohanty, B.; Katti, D. R. *J. Mater. Res.* **2006**, *21*, 1237.
(3) Wang, R. Z.; Suo, Z.; Evans, A. G.; Yao, N.; Aksay, I. A. *J. Mater. Res.* **2001**, *16*, 2485.
(4) Taylor, J. D.; Kennedy, W. J.; Hall, A. *Bull. Br. Mus.* **1969**, *125*, 3.
(5) Currey, J. D. *Proc. R. Soc. London* **1977**, *196*, 443.
(6) Katti, K. S.; Katti, D. R.; Pradhan, S. M.; Bhosle, A. *J. Mater. Res.* **2005**, *20*, 1097.
(7) Wada, K. *Biomineralisation* **1972**, *6*, 141.
(8) Katti, D. R.; Pradhan, S. M.; Katti, K. S. *J. Rev. Adv. Mater. Sci.* **2004**, *n6*, 162.
(9) Jordinades, X. J.; Lang, M. J.; Song, X.; Fleming, G. R. *J. Phys. Chem. B* **1999**, *103*, 7995.
(10) Pal, S. K.; Mandal, D.; Sukul, D.; Sen, S.; Bhattacharyya, K. *J. Phys. Chem. B* **2001**, *105*, 1438.

(11) Joo, T.; Jia, Y.; Yu, J. U.; Lang, M. J.; Song, X.; Fleming, G. R. *J. Chem. Phys.* **1996**, *104*, 6089.
(12) Pal, S. K.; Peon, J.; Zewail, A. H. *Proc. Natl. Acad. Sci. U.S.A.* **2002**, *99*, 1763.
(13) Rasche, T. M.; Tsai, J.; Levitt, M. *Proc. Natl. Acad. Sci. U.S.A.* **2001**, *98*, 5965.
(14) Bandyopadhyay, S.; Chakraborty, S.; Balasubramanian, S.; Pal, S. Bagchi, B. *J. Phys. Chem. B* **2004**, *108*, 12608.
(15) Mohanty, B.; Katti, K. S.; Katti, D. R. *J. Mater. Res.* **2006**, *21*, 2045.
(16) Verma, D.; Katti, K. S.; Katti, D. R. *Spectrochim. Acta* **2006**, *64*, 1051.
(17) Verma, D.; Katti, K. S.; Katti, D. R. *Spectrochim. Acta*, in press.
(18) de Villers, J. P. R. *Am. Mineral.* **1971**, *5*, 758.
(19) Phillips, J. C.; Braun, R.; Wang, W.; Gumbart, J.; Tajkhorshid, E.; Villa, E.; Chipot, C.; Skeel, R.; Kale, L.; Schulten, K. *J. Comput. Chem.* **2005**, *26*, 1781.
(20) Zentz, F.; Bedouet, L.; Almeida, M. J.; Milet, C.; Lopez, E.; Giraud, M. *Mar. Biotechnol.* **2001**, *3*, 36.
(21) Weiss, I. M.; Renner, C.; Strigl, M. G.; Fritz, M. *Biochem. Biophys. Res. Commun.* **2001**, *285*, 244.
(22) Levi, Y.; Albeck, S.; Brack, A.; Weiner, S.; Addadi, L. *Chem.-Eur. J.* **1998**, *4*, 389.
(23) Falini, G.; Albeck, S.; Brack, A.; Weiner, S.; Addadi, L. *Science* **1996**, *271*, 67.
(24) Walters, D. A.; Smith, B. L.; Belcher, A. M.; Paloczi, G. T.; Stucky, G. D.; Morse, D. E.; Hansma, P. K. *Biophys. J.* **1997**, *72*, 1425.
(25) Schäffer, T. E.; Ionescu-Zanetti, C.; Proksch, R.; Fritz, M.; Walters, D. A.; Almqvist, N.; Zaremba, C. M.; Belcher, A. M.; Smith, B. L.; Stucky, G. D.; Morse, D. E.; Hansma, P. K. *Chem. Mater.* **1997**, *9*, 1731.
(26) Smith, B. L.; Schaffer, T.; Viani, M.; Thompson, J. B.; Frederick, N. A.; Kindt, J.; Belcher, A. M.; Stucky, G. D.; Morse, D. E.; Hansma, P. K. *Nature* **1999**, *399*, 761.
(27) Shen, X.; Belcher, A. M.; Hansma, P. K.; Stucky, G. D.; Morse, D. E. *J. Biol. Chem.* **1997**, *272*, 32472.
(28) Hohl, D.; Mehrel, T.; Lichti, U.; Turner, M. L.; Roop, D. R.; Steinert, P. M. *J. Biol. Chem.* **1991**, *266*, 6626.
(29) Zhang, B.; Wustman, A.; Morse, D.; Spencer, J. E. *Biopolymers* **2002**, *6*, 358.
(30) Humphrey, W.; Dalke, A.; Schulten, K. *J. Mol. Graphics* **1996**, *14*, 33; http://www.ks.uiuc.edu/Research/vmd/.
(31) Gao, M.; Craig, D.; Lequin, O.; Campbell, I. D.; Vogel, V.; Schulten, S. *Proc. Natl. Acad. Sci. U.S.A.* **2003**, *100*, 14784.
(32) Vazquez, M. C.; Li, H.; Lu, H.; Marszalek, P. E.; Oberhauser, A. F.; Fernandez, J. M. *Nat. Struct. Biol.* **2003**, *10*, 738.
(33) Gao, M.; Craig, D.; Vogel, V.; Schulten, K. *J. Mol. Biol.* **2002**, *323*, 939.
(34) Brooks, B. R.; Bruccoleri, R. E.; Olafson, B. D.; Swaminathan, D. S.; Karplus, M. *J. Comput. Chem.* **1983**, *4*, 187.

BM060942H